Special Cases during the Detection of the Hook Style Energy Theft in Overhead Low-Voltage Power Grids through HS-DET Method – Part 2: Different Measurement Differences, Feint "Smart" Hooks and Hook Interconnection Issues

Athanasios G. Lazaropoulos*

School of Electrical and Computer Engineering / National Technical University of Athens / 9 Iroon Polytechniou Street / Zografou, GR 15780

Received November 01, 2018; Accepted December 18, 2018; Published December 26, 2018

On the basis of [1] and [2], this paper investigates the possibility of jamming the method of the detection of the hook style energy theft (HS-DET method) that is used for the detection of the hook style energy theft in the overhead low-voltage (OV LV) power grids. Three more sophisticated scenarios, which have been revealed in [2] and are the evolution of the three main suspicious issues of [1], are further investigated in this paper. The detection efficiency of HS-DET method is assessed by using the already validated percent error sum (PES) submetrics and appropriate contour plots.

Keywords: Smart Grid; Broadband over Power Lines (BPL); Power Line Communications (PLC); Distribution Power Grid; Energy Theft; Jamming; Robustness

1. Introduction

The hook style energy theft detection method (HS-DET method), which has been proposed in [1] and partially tested on its detection performance during a set of special cases in [2], aims at detecting the hook style energy theft in overhead low-voltage (OV LV) power grids that exploit broadband over powerlines (BPL) technology conveniences. HS-DET method is added in the existing portfolio of BPL broadband applications, such as Topology Identification Methodology (TIM) [3], Fault and Instability Identification Methodology (FIIM) [4], methodology to preserve power system stability [5], [6] and main line fault localization methodology (MLFLM) [7]-[9], while its application is considered valid when all the problematic cases of TIM, FIIM and MLFLM are excluded. The portfolio of BPL broadband applications focuses on a more accurate and more reliable monitoring, metering and controlling of distribution power grids.

HS-DET method is based on the hybrid model [10]-[27] while the hook style energy theft is detected by HS-DET method through $\overline{\Delta PES}$ metric, which is the suitable percent error sum (PES) submetric for energy theft detection, and its relevant contour plots. Actually, $\overline{\Delta PES}$ evaluates the asymmetry between the original and the modified

Corresponding author: AGLazaropoulos@gmail.com

Tr Ren Energy, 2019, Vol.5, No.1, 90-116. doi: 10.17737/tre.2019.5.1.0083

OV LV BPL topology where the modified OV LV BPL topology comes from the original OV LV BPL topology after the hook insertion. If $\overline{\Delta PES}$ remains above the strict $\overline{\Delta PES}$ threshold, which is equal to 10%, a safe detection of a hook style energy theft can be received. If $\overline{\Delta PES}$ remains between the above the loose $\overline{\Delta PES}$ threshold, which is equal to 0%, and the strict $\overline{\Delta PES}$ threshold, a less safe detection of a hook style energy theft can be received. Here, it should be noted that HS-DET method can give reliable decisions concerning the existence of the energy theft regardless of the existence of very intense measurement differences due to the $\overline{\Delta PES}$ definition that can significantly mitigate them (see [1] and Appendix of [2]).

In accordance with [1], three special issues have been addressed there and it has been proven in [2] that these three special issues cannot jam HS-DET method. More specifically, the concluding remarks concerning these three special issues can be synopsized as: (i) There is no threshold of CUD maximum values $a_{\mathbf{CUD}}$ of measurement differences below 20 dB that HS-DET method could not detect the hook style energy theft; (ii) The installation of very long hooks in order to mask the hook existence during the application of HS-DET method can indeed make the energy theft detection less easy by HS-DET method but again in all the cases HS-DET method can detect the hook style energy theft through its strict and loose $\overline{\Delta PES}$ thresholds; and (iii) The $\overline{\Delta PES}$ behavior of "smart" hook technique resembles to the respective behavior of very long hooks and hence the energy theft detection of "smart" hook technique by HS-DET method remains as easy as in the very long hook technique. In all the three special issues, HS-DET method detected the energy theft through strict and loose $\overline{\Delta PES}$ thresholds.

In accordance with [2], three more sophisticated scenarios have been proposed that aspire, by exploiting and extending the strengths of the three special cases, to distract further HS-DET method. With reference to [1] and [2], these three sophisticated scenarios are: (a) the existence of different CUD measurement differences of the same maximum value $a_{\mathbf{CUD}}$ when the coupling transfer functions of the original and the modified OV LV BPL topologies are measured; (b) The installation of a second "smart" hook, which acts as a feint device, so that the first "smart" hook that is responsible for the energy theft can be camouflaged; and (c) The impact of the full interconnection assumption of the "smart" hook during the computations of HS-DET method.

The rest of this paper is organized as follows: In Section 2, numerical results and discussion are provided, aiming at practically evaluating the efficiency of the three sophisticated scenarios towards the jamming of HS-DET method. Section 3 concludes this paper.

2. Numerical Results and Discussion

The numerical results of this Section focus on assessing the performance of HS-DET method and describe the behavior of HS-DET method when the aforementioned three sophisticated scenarios occur. All these three scenarios try to jam HS-DET method, each one exploiting its own strengths presented in [2]. For that reason, the robustness of decisions of HS-DET method is also evaluated as well as the road map towards safer decisions concerning the detection of hook style energy thefts. As the circuital, topological and coupling scheme characteristics of OV LV BPL networks are concerned, these remain the same with [1], [2].

2.1 Different CUD Measurement Differences and HS-DET Method Jamming

The influence of measurement differences of maximum value a_{CUD} up to 5 dB has been thoroughly discussed in [1] while the influence of measurement differences of maximum value a_{CUD} above 5 dB has been evaluated in [2]. It has been proven that there is no threshold of CUD maximum values a_{CUD} of measurement differences below 20 dB that HS-DET method could not detect the hook style energy theft. Actually, in the vast majority of the cases examined, HS-DET method detected the energy theft through its strict $\overline{\Delta PES}$ threshold while the loose $\overline{\Delta PES}$ threshold of HS-DET method have been used in special cases such as urban OV LV BPL topologies when very high measurement differences occur.

With reference to eqs. (2)-(4) of [2], HS-DET method can successfully detect the hook style energy theft regardless of the CUD maximum values a_{CUD} of measurement differences when measurements of original measured coupling scheme channel transfer function and modified measured coupling scheme channel transfer functions are available at the same time. However, the cost of a non-real time and continuous HS-DET method in terms of $\overline{\Delta PES}$ is going to be assessed in this subsection.

If simultaneous measurements of original measured coupling scheme channel transfer function and modified measured coupling scheme channel transfer functions are not available, the aforementioned measured transfer functions suffer from different measurement differences. Supposing that the environmental and circuital conditions of the examined OV LV power grid remain the same due the short time interval between the two measurements, two different CUD measurement differences of the same maximum values a_{CUD} affect the original measured coupling scheme channel transfer function and the modified measured coupling scheme channel transfer functions. In this paper, the influence of average measurement differences (*i.e.,* measurement differences of maximum value a_{CUD} between 0 dB and 5 dB) is evaluated in this paper. In accordance with [2], the performance of HS-DET method against different measurement differences will be assessed in terms of $\overline{\Delta PES}$, $\overline{PES_{\mathrm{or}}}$ and $\overline{Rob}$.

With reference to Fig. 2(b) of [1] and the indicative original OV LV BPL topologies as reported in Table 1 of [1], let assume that a hook of length L_{bh} is inserted at distance D_{h} from the transmitting end. In Fig. 1(a), $\overline{\Delta PES}$ is plotted with respect to the maximum value a_{CUD} when $L_{\mathrm{bh}} = 5\mathrm{m}$ and $D_{\mathrm{h}} = 300\mathrm{m}$ are assumed for the five indicative original OV LV BPL topologies. Note that two different CUD measurement differences are used during the determination of the original measured coupling scheme channel transfer function and the modified measured coupling scheme channel transfer functions. In Figs. 1(b) and 1(c), same curves with Fig. 1(a) are given but for $\overline{PES_{\mathrm{or}}}$ and $\overline{Rob}$, respectively.

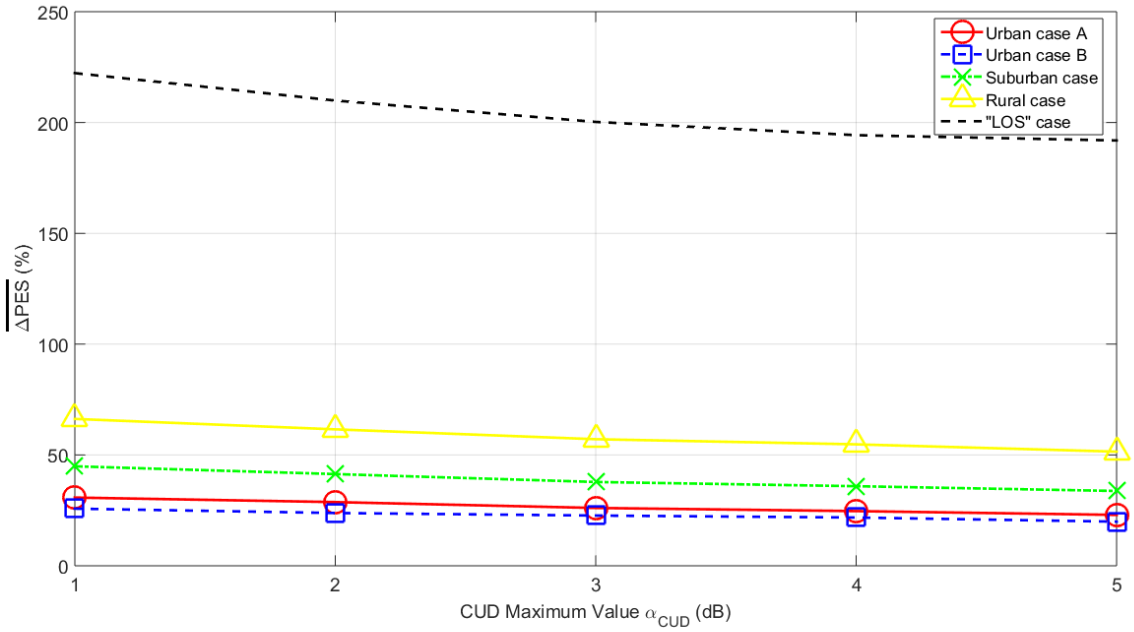
Urban case A
Urban case B
Suburban case
Rural case
"LOS" case
ΔPES (%)
CUD Maximum Value α_{CUD} (dB)

(a)

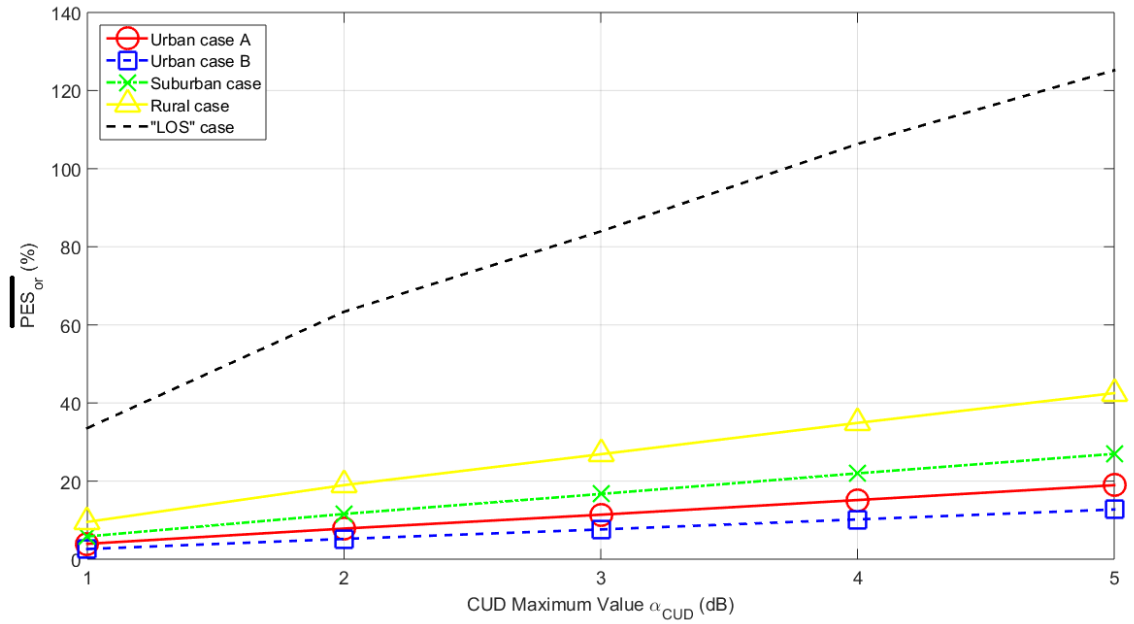
Urban case A
Urban case B
Suburban case
Rural case
"LOS" case
PES_{or} (%)
CUD Maximum Value α_{CUD} (dB)

(b)

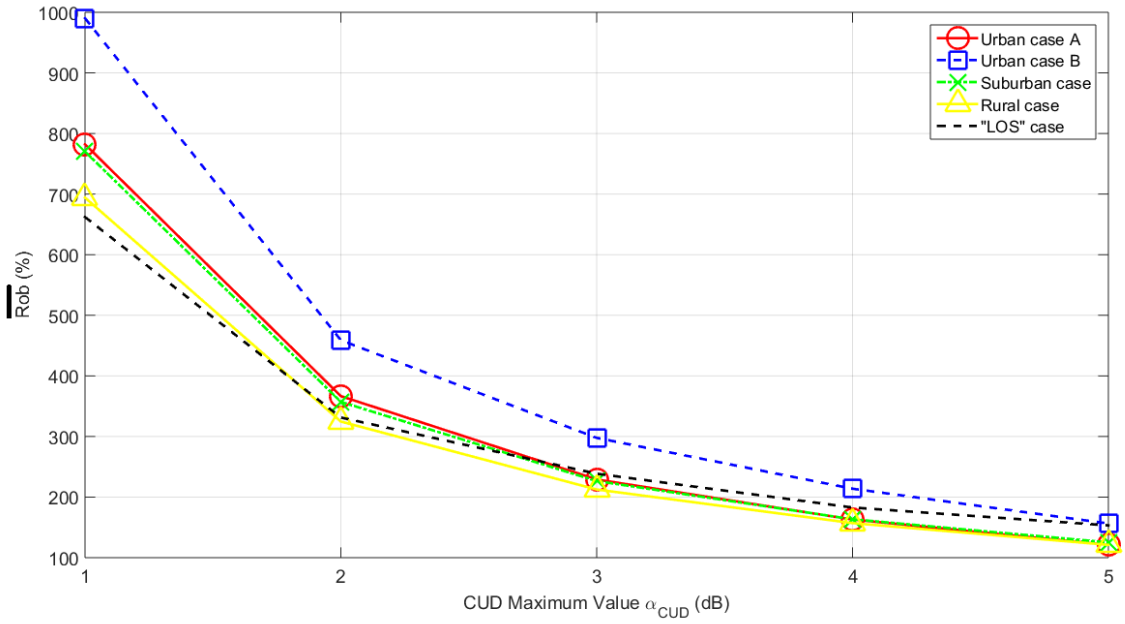

(c)

Fig. 1. PES submetrics of HS-DET method for the five original indicative OV LV BPL topologies of [1] when hook length of 5 m, hook distance from the transmitting end of 300 m and open-circuit hook termination are assumed for two different CUD measurement differences and various maximum values a_{CUD}. (a) $\overline{\Delta PES}$. (b) $\overline{PES_{or}}$. (c) $\overline{Rob}$.

From Figs. 1(a)-(c), it is evident that HS-DET method can easily detect the hook style energy theft even if unintentional / intentional different measurement differences occur during the determination of the original measured coupling scheme channel transfer function and the modified measured coupling scheme channel transfer functions. This easily can be explained since all $\overline{\Delta PES}$ and $\overline{Rob}$ values of all the indicative OV LV BPL topologies remain well above the respective $\overline{\Delta PES}$ and $\overline{Rob}$ strict thresholds, which have been described in [2] (*i.e.,* strict $\overline{\Delta PES}$ and $\overline{Rob}$ thresholds are assumed to be equal to 10% and 20%, respectively).

In accordance with [2], the three categories of OV LV BPL topologies concerning the hook style energy theft detection through $\overline{\Delta PES}$, say, "LOS", good channel and bad channel cases, also remain the same despite the different CUD measurement differences. Similarly to the case of common CUD measurement differences during the determination of the original measured coupling scheme channel transfer function and the modified measured coupling scheme channel transfer functions, the easiest decision concerning the energy theft detection remains in original "LOS" case while the most precarious one remains in the bad channel case.

Although the detection of the energy theft is based on the strict $\overline{\Delta PES}$ and $\overline{Rob}$ thresholds in all the examined OV LV BPL topologies and CUD maximum values, the uncertainty degree of the two different CUD measurement differences, which is intrinsically added in the $\overline{\Delta PES}$ and $\overline{Rob}$ curves of respective Figs. 1(a) and 1(c), need to be assessed. This assessment will highlight the possibility of jamming the decision concerning the energy theft. In Appendix, the sole influence of the two different CUD measurement differences of the same maximum value a_{CUD} is assessed in terms of $\overline{\Delta PES}$,

$\overline{PES_{or}}$ and $\overline{Rob}$. As it is shown in the Appendix, the effect of two different CUD measurement differences on $\overline{\Delta PES}$ and $\overline{Rob}$ values remains marginal (*i.e.,* below 3% and 4% for $\overline{\Delta PES}$ and $\overline{Rob}$, respectively) and remain as a small fraction of the respective $\overline{\Delta PES}$ and $\overline{Rob}$ values in all the cases examined in Figs. 1(a) and 1(c). However, the effect of two different CUD measurement differences on $\overline{\Delta PES}$ and $\overline{Rob}$ values cannot be neglected in the cases where the decision concerning the existence of hook style energy theft needs to be taken by using the respective loose $\overline{\Delta PES}$ and $\overline{Rob}$ thresholds (see decisions with loose $\overline{\Delta PES}$ and $\overline{Rob}$ thresholds in [2]).

Since the impact of two different CUD measurement differences on the detection of hook style energy theft is negligible in the cases examined in this paper, a common CUD measurement difference during the determination of the original theoretical coupling scheme channel transfer function and the modified theoretical coupling scheme channel transfer function is considered in the following analysis. Anyway, this is the typical procedure that has been followed until now and further implies the existence of a real time and continuous HS-DET method.

Also, by comparing Figs. 1(a) and 1(c), there are no areas of maximum value a_{CUD} uncertainty where $\overline{\Delta PES}$ and $\overline{Rob}$ give conflicting results concerning the existence of hook style energy theft. Therefore, only $\overline{\Delta PES}$ plots are going to be used in the following analysis.

2.2 Two “Smart” Hooks and HS-DET Method Jamming

In accordance with [2], the installation of additional equipment on the power grid can be easily detectable by the authorized maintenance personnel. However, the small size of “smart” hooks can be camouflaged in comparison with other energy theft techniques such as the very long hooks technique. Anyway, HS-DET method can detect any hook style energy theft that is based on the concept of “smart” hooks but in few cases such as the aggravated urban OV LV BPL topologies that suffer from intentional / unintentional measurement differences, the detection has been made through the loose $\overline{\Delta PES}$ threshold [2].

The concept of this subsection is that the use of two “smart” hooks, where the first one (hook A) will perform the energy theft and the second one (hook B) will try to jam HS-DET method as a feint hook, could significantly decrease $\overline{\Delta PES}$ values. As indicated in Sec.2.1, the success of this combined use of “smart” hooks would be accomplished if $\overline{\Delta PES}$ values can remain below 5%. Although $\overline{\Delta PES}$ values that are below 5% can be detected by the loose $\overline{\Delta PES}$ threshold, these $\overline{\Delta PES}$ values can be considered as various small measurement differences, which have not been mitigated and finally ignored by the authorized maintenance personnel. Anyway, $\overline{\Delta PES}$ values that are below 5% have been detected neither in [1] nor in [2] in all the cases examined.

To investigate the possibility of camouflaging the hook style energy theft through the use of two “smart” hooks, in Fig. 2(a), $\overline{\Delta PES}$ is plotted versus the hook A distance from the transmitting end and the hook B distance from the transmitting end when the OV LV BPL topology of urban case A is assumed, and maximum value a_{CUD} of 1 dB is applied. In Figs. 2(b) and 2(c), same contour plots with Fig. 2(a) are given but for maximum value a_{CUD} of 2 dB and 5 dB, respectively. In Figs. 3, 4, 5 and 6, same plots with Fig. 2 are given but for the case of the urban case B, suburban case, rural case and “LOS” case, respectively. In accordance with [1], the hook A and B distance from the transmitting end span is assumed to be equal to 50 m, the terminations of hook A and B

are assumed to be matched while the hook A and B length is assumed to be equal to 5m for all the examined contour plots of this paper. Note that the range of the hook A distance from the transmitting end is from 1 m to 951 m for all the examined contour plots of this paper while the respective range of the hook B is from 2 m to 952 m.

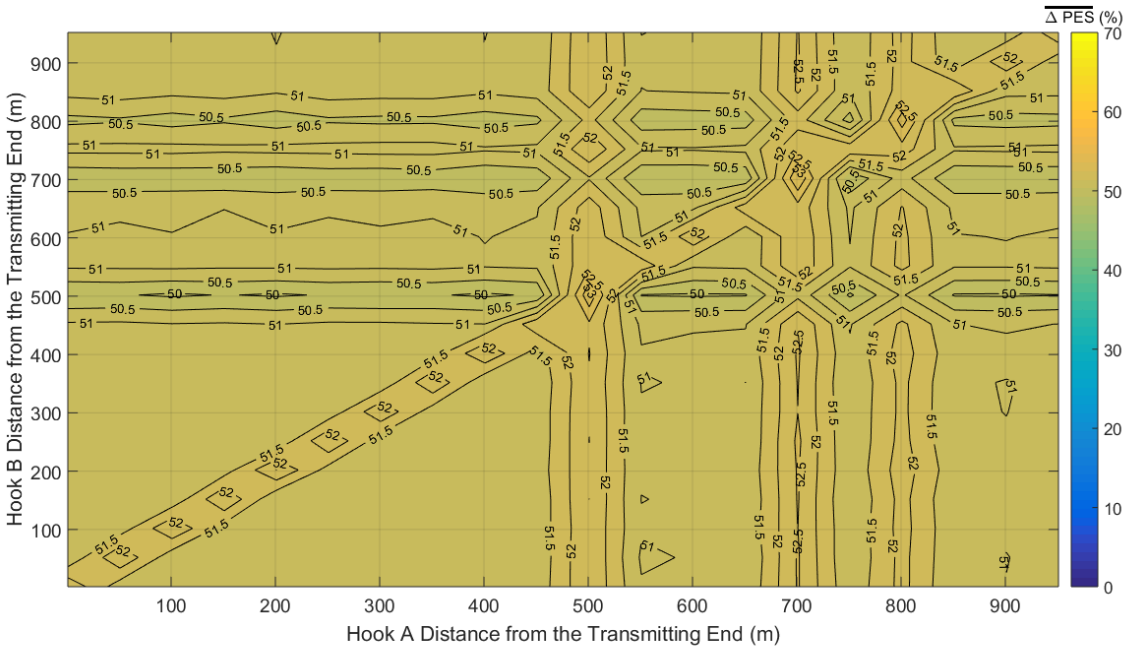

(a)

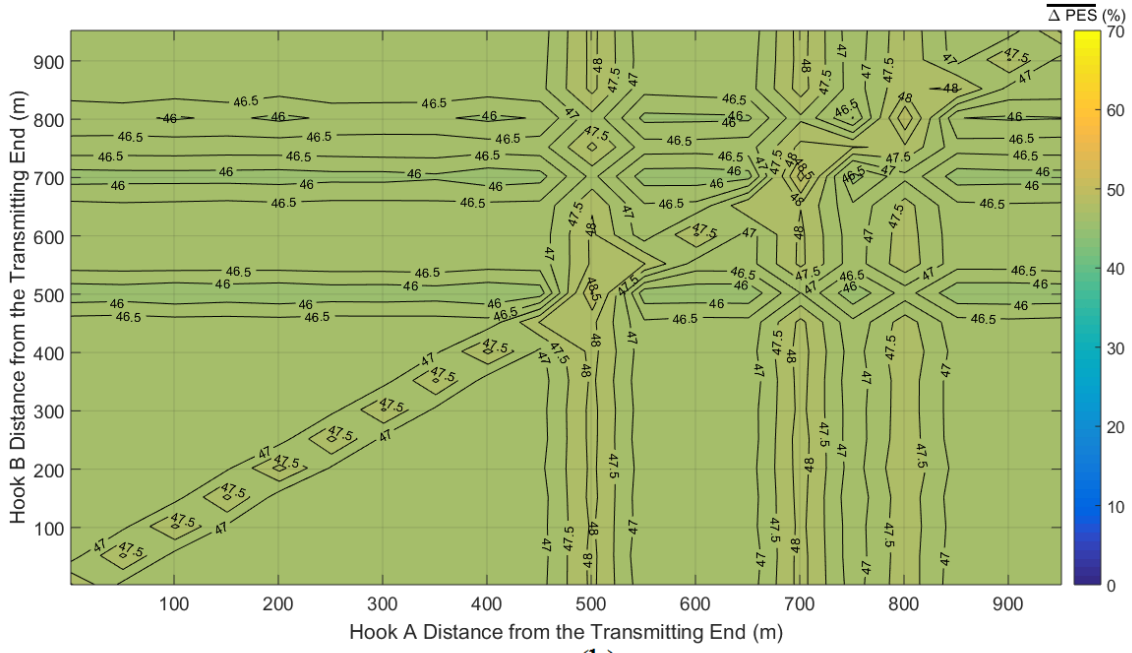

(b)

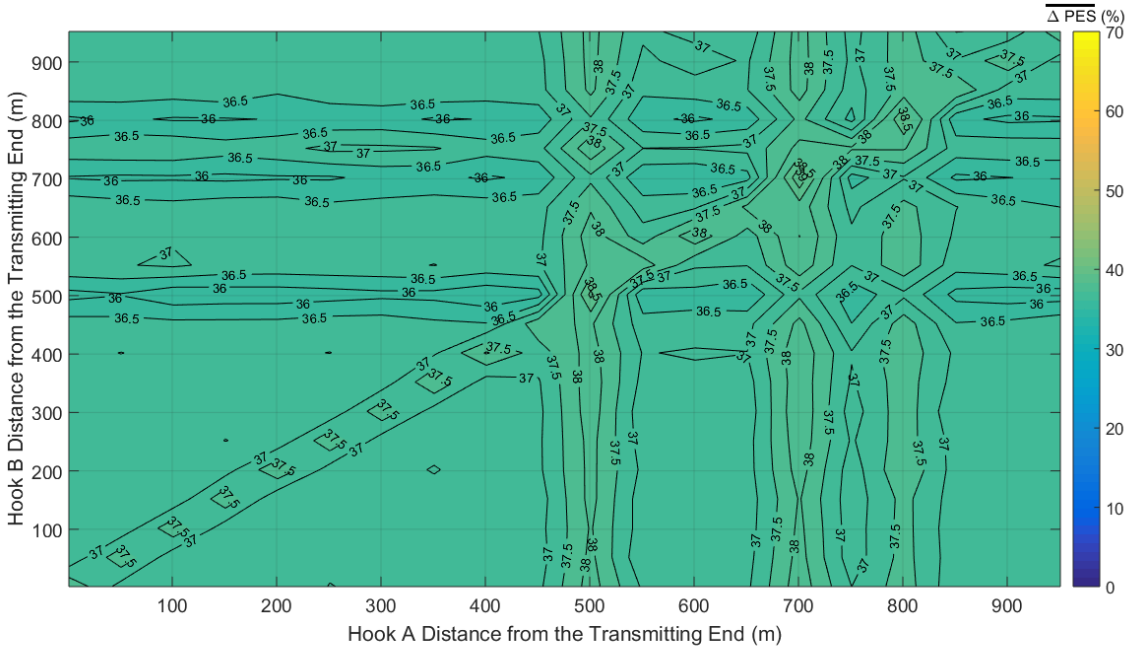

(c)

Fig. 2. $\overline{\Delta PES}$ of the urban case A of the indicative OV LV BPL topologies in the 3-88MHz frequency band for various hook A and hook B distances from the transmitting end. (a) $a_{CUD} = 1\text{dB}$. (b) $a_{CUD} = 2\text{dB}$. (c) $a_{CUD} = 5\text{dB}$.

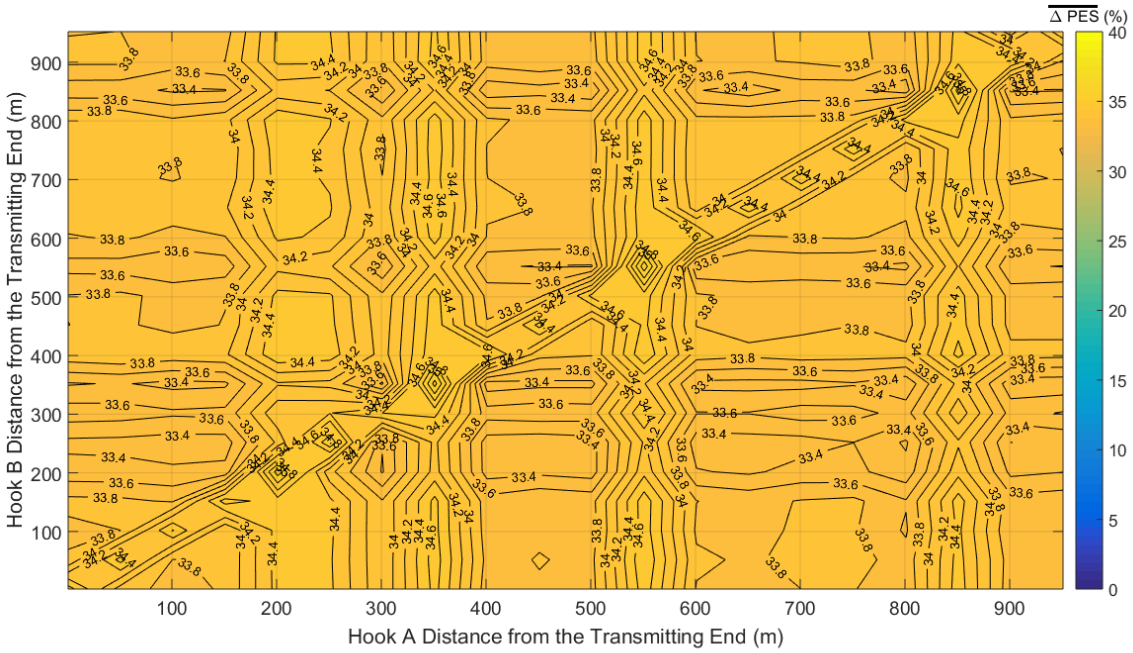
Δ PES (%)
Hook B Distance from the Transmitting End (m)
Hook A Distance from the Transmitting End (m)

(a)

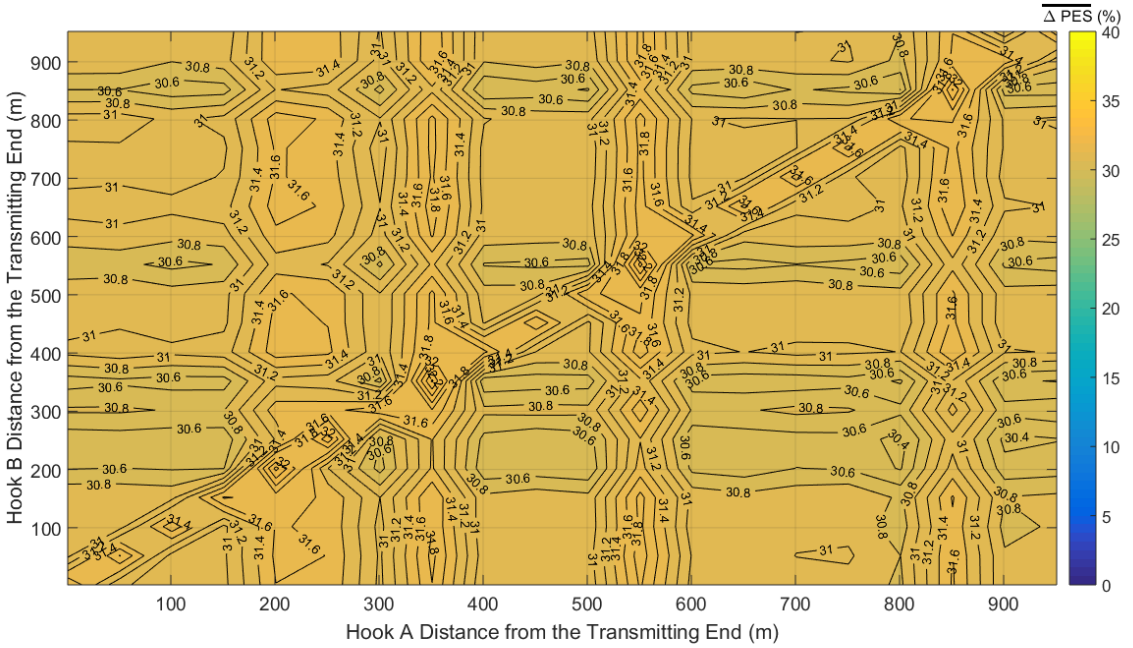
Δ PES (%)
Hook B Distance from the Transmitting End (m)
Hook A Distance from the Transmitting End (m)

(b)

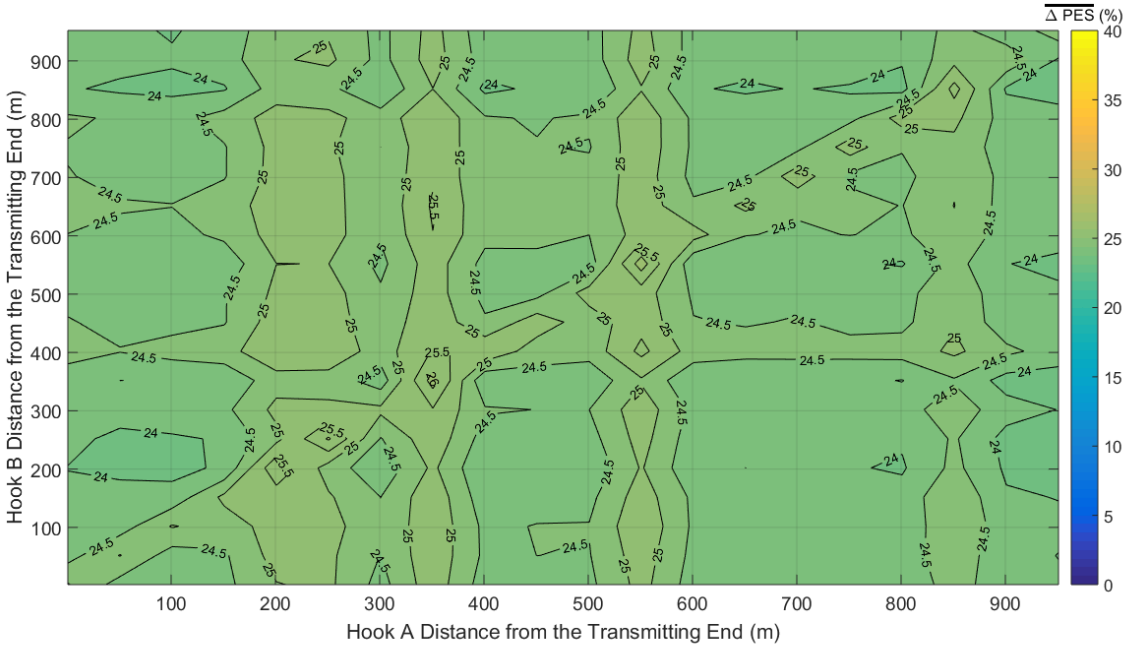

(c)

Fig. 3. Same curves with Fig. 2 but for the urban case B.

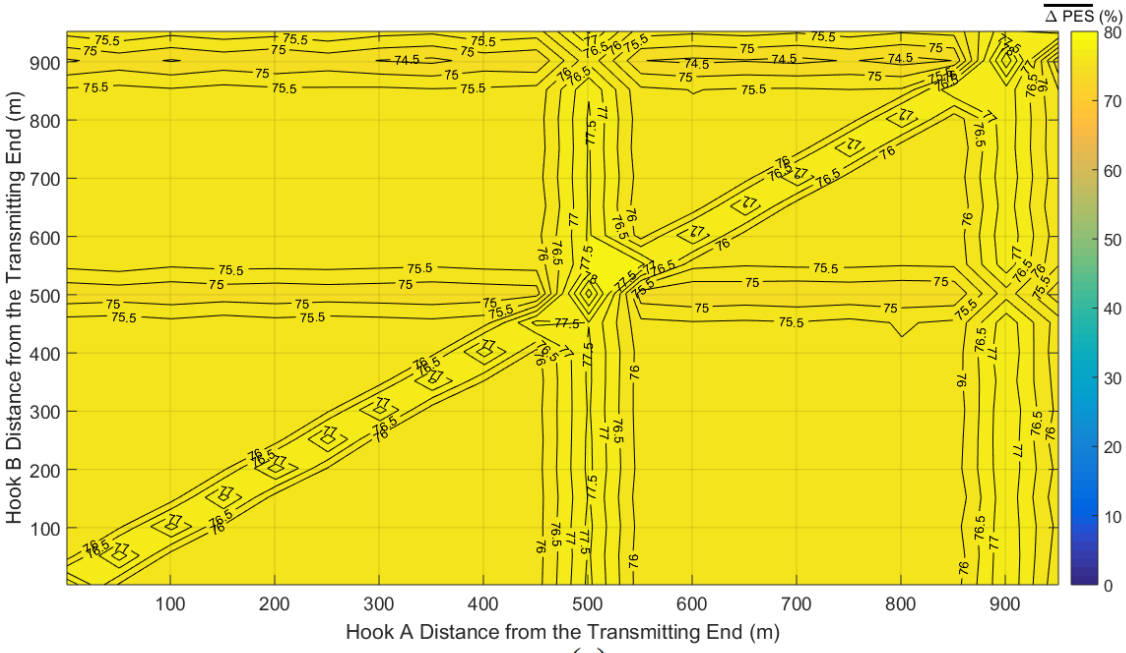
Δ PES (%)
Hook B Distance from the Transmitting End (m)
Hook A Distance from the Transmitting End (m)

(a)

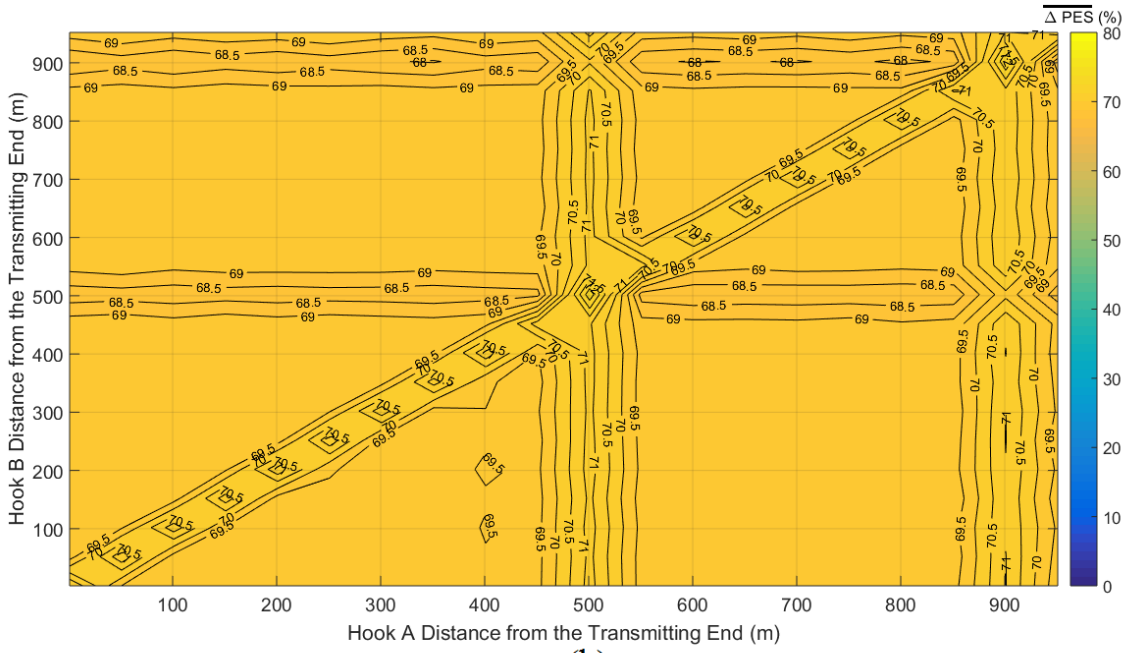
Δ PES (%)
Hook B Distance from the Transmitting End (m)
Hook A Distance from the Transmitting End (m)

(b)

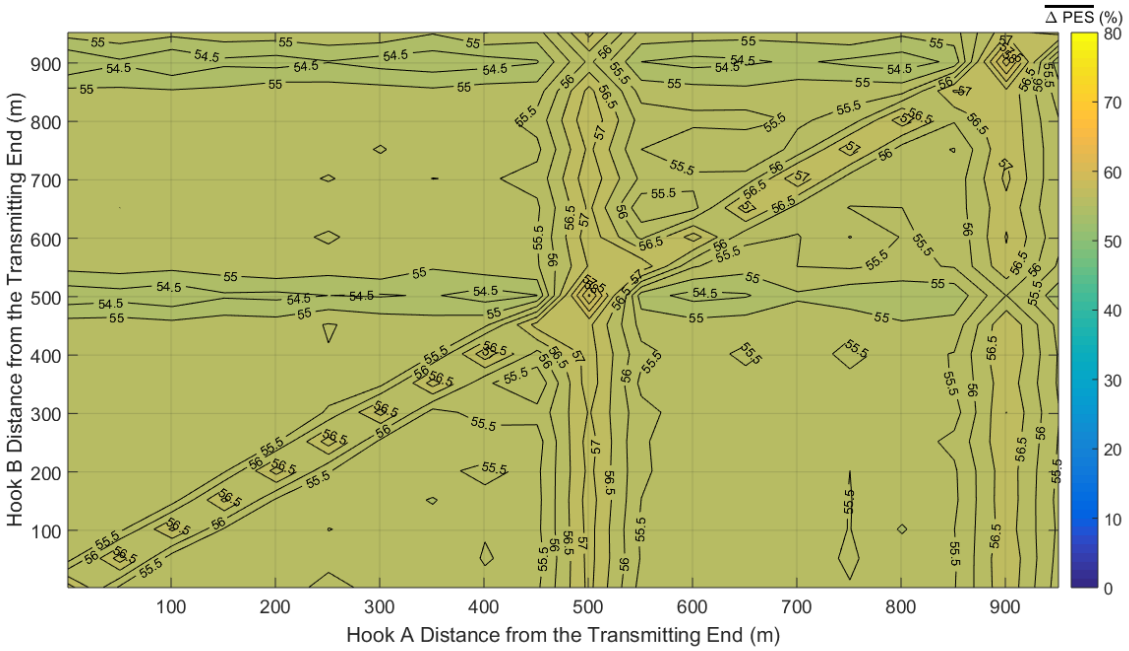

(c)

Fig. 4. Same curves with Fig. 2 but for the suburban case.

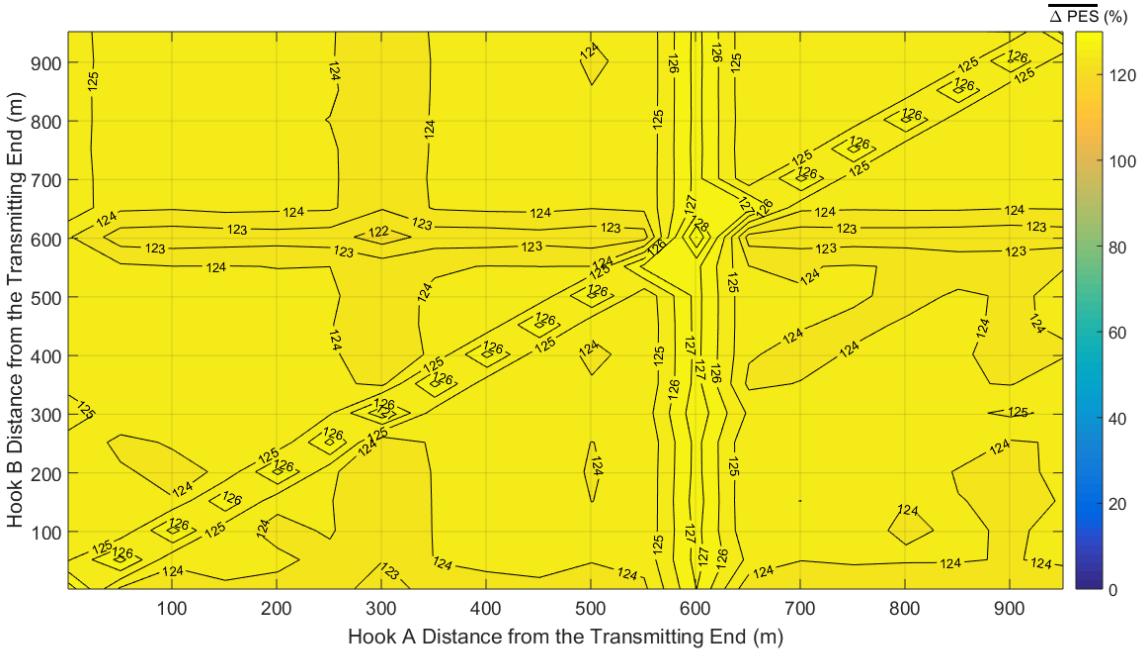
Δ PES (%)
Hook B Distance from the Transmitting End (m)
Hook A Distance from the Transmitting End (m)

(a)

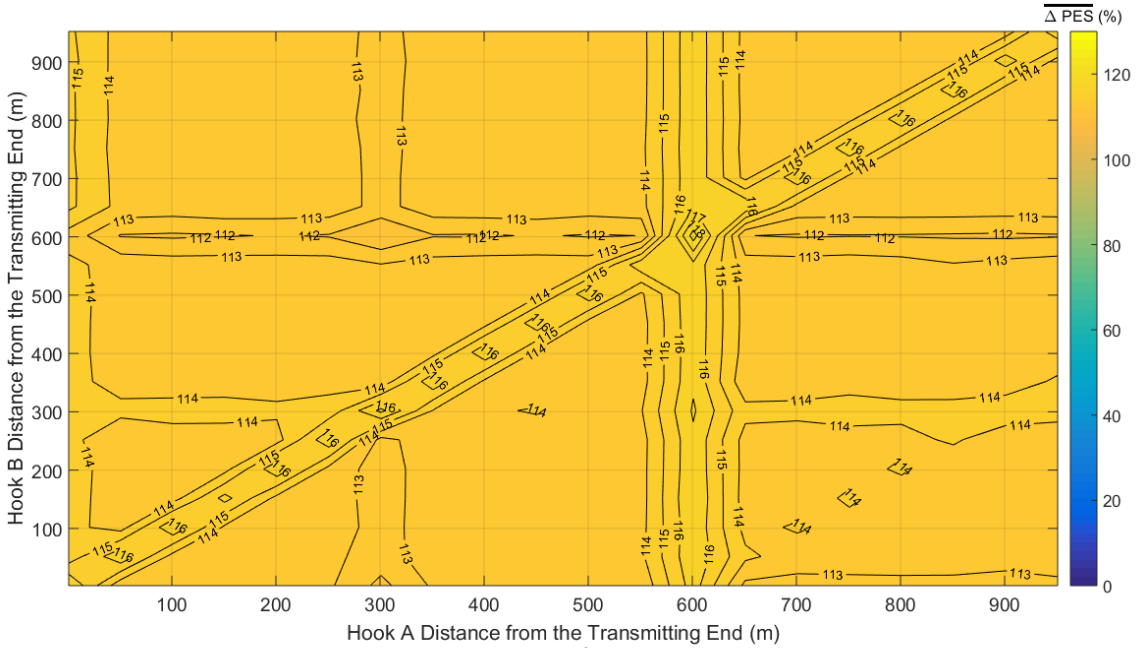
Δ PES (%)
Hook B Distance from the Transmitting End (m)
Hook A Distance from the Transmitting End (m)

(b)

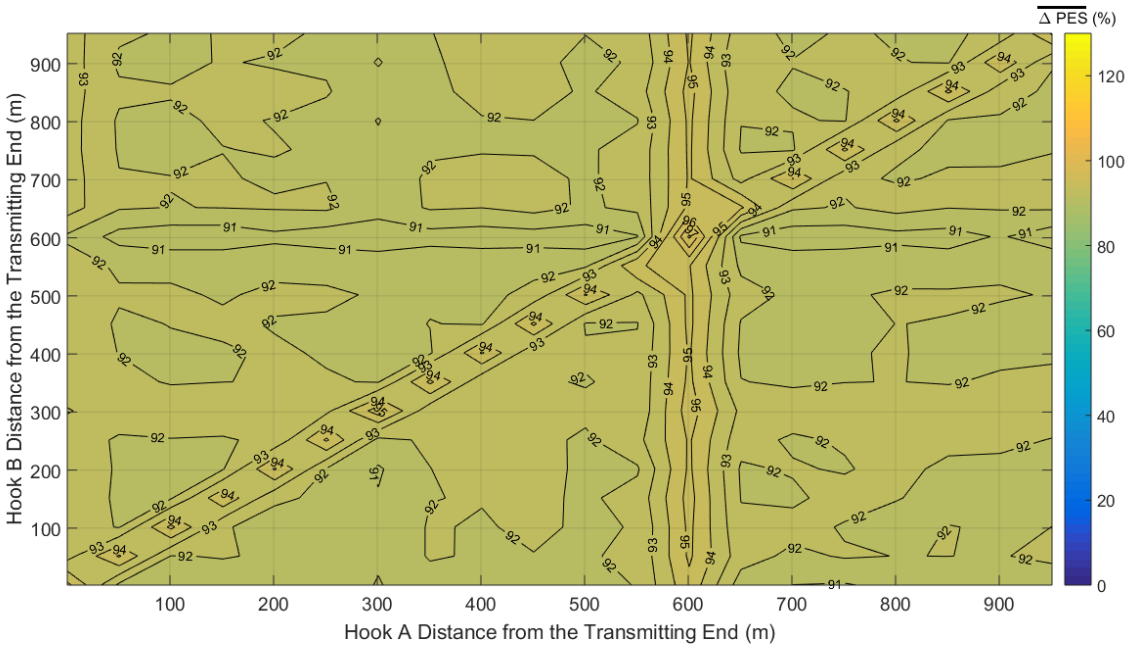

(c)

Fig. 5. Same curves with Fig. 2 but for the rural case.

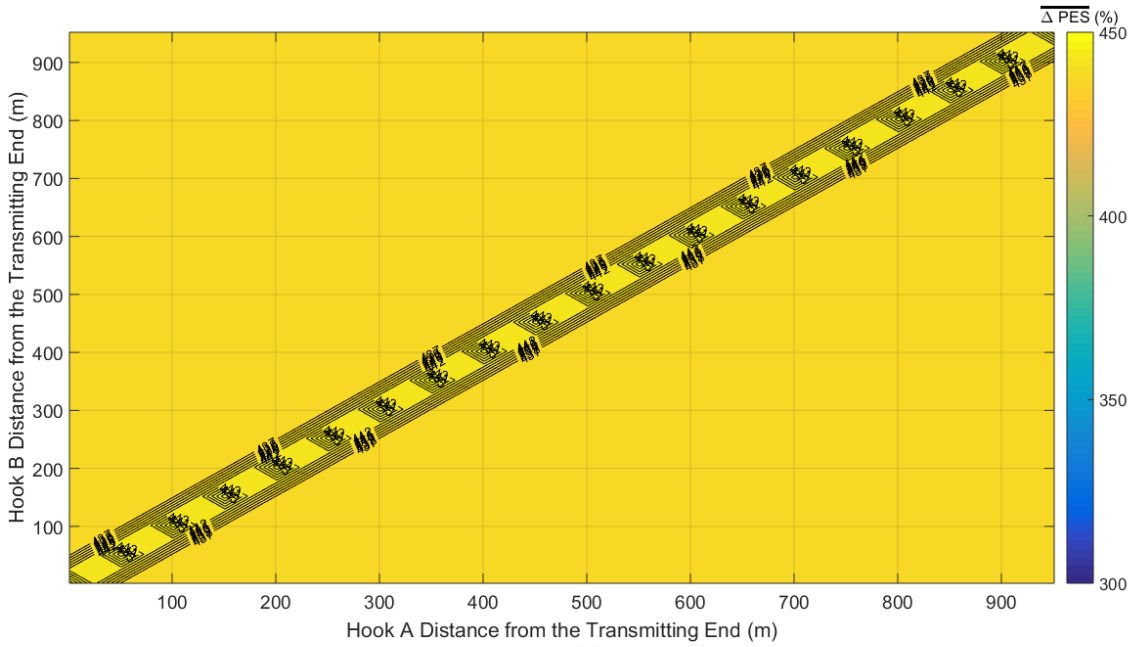
Δ PES (%)
450
400
350
300
Hook B Distance from the Transmitting End (m)
100
200
300
400
500
600
700
800
900
Hook A Distance from the Transmitting End (m)

(a)

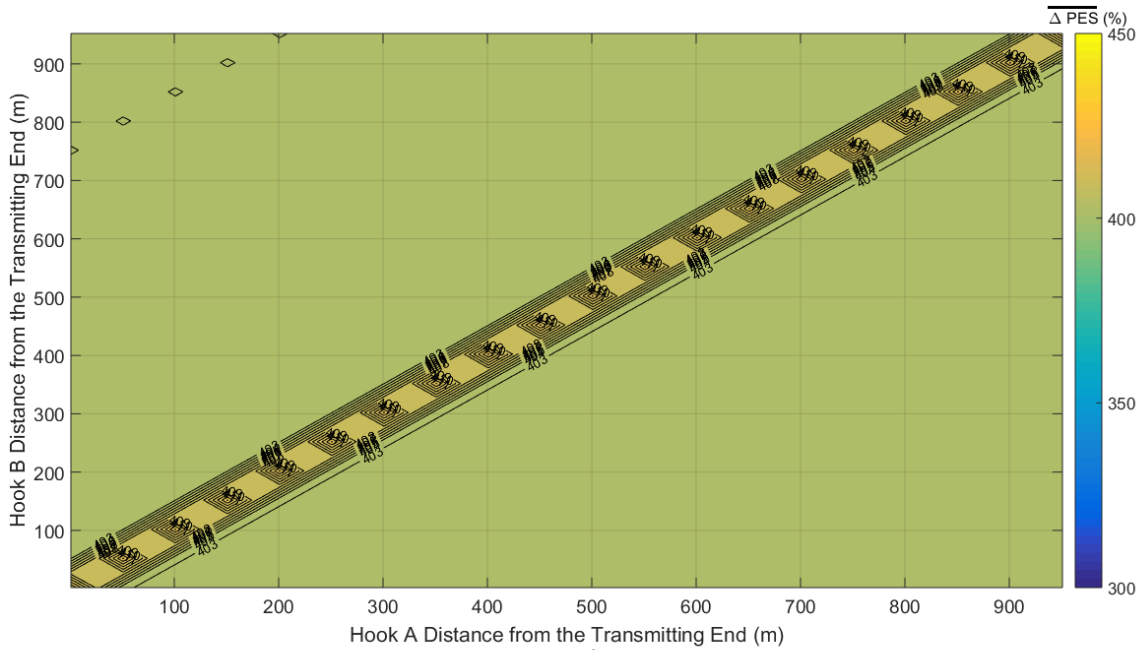
Δ PES (%)
450
400
350
300
Hook B Distance from the Transmitting End (m)
100
200
300
400
500
600
700
800
900
Hook A Distance from the Transmitting End (m)

(b)

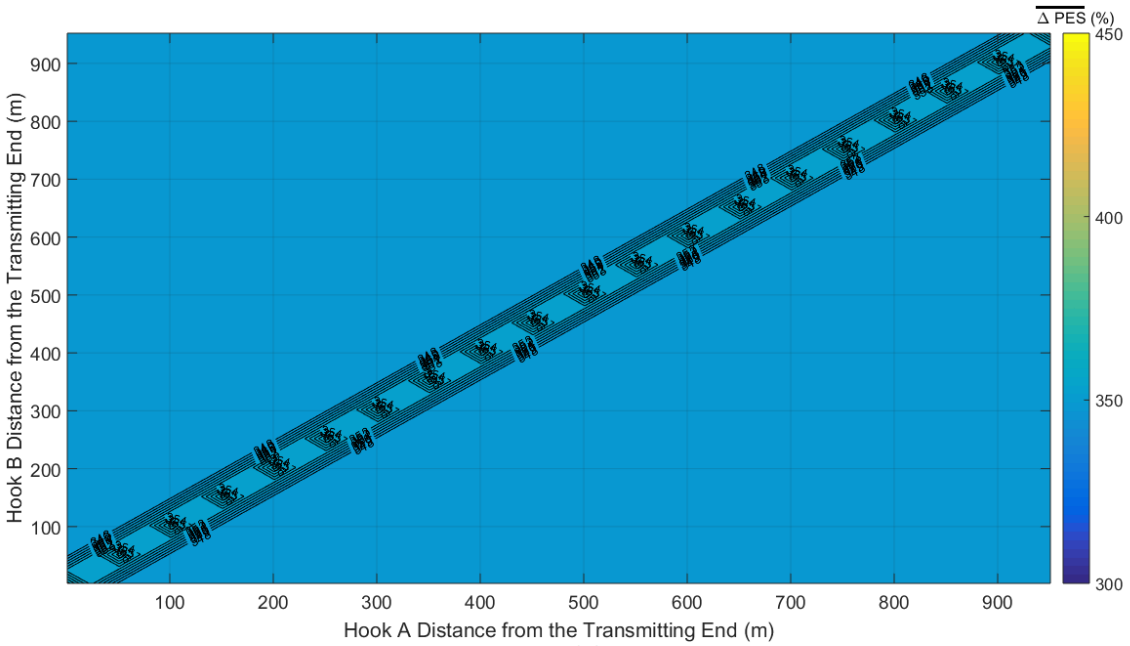

(c)

Fig. 6. Same curves with Fig. 2 but for the "LOS" case.

From Figs. 2-6, the insertion of the feint "smart" hook significantly increases $\overline{\Delta PES}$ values for given OV LV BPL topology, "smart" hook A distance from the transmitting end and maximum value a_{CUD}. Instead of reducing $\overline{\Delta PES}$ values, HS-DET method now more easily detects the energy theft; when the feint "smart" hook is employed, $\overline{\Delta PES}$ values of Figs. 2-6 are more than twice as high as those of the respective Figs. 2-6 of [2] in all the cases examined. In addition, higher $\overline{\Delta PES}$ values are observed when two "smart" hooks remain close enough due to the fact that the comparable distance of two hooks allows the creation of new significant multipath channels [10], [12]. Furthermore, $\overline{\Delta PES}$ difference between the highest and lowest $\overline{\Delta PES}$ value for given figure remains below 3% in all the cases examined.

In addition, each of Figs. 2-6 presents a strong symmetry with respect to the diagonal linking the top of the axes with the top right top. This implies that the overall $\overline{\Delta PES}$, which is shown in Figs. 2-6, can be regarded as the additive result of the partial $\overline{\Delta PES}$ of the two "smart" hooks.

Anyway, by comparing Figs. 2-6 with Fig. 7(a) of [2], it is clear that the two-"smart"-hooks technique cannot jam HS-DET method by its own. Actually, the effect of feint "smart" hook on $\overline{\Delta PES}$ values can be described as a small $\overline{\Delta PES}$ fluctuation to the existing $\overline{\Delta PES}$ values of the first "smart" hook while the effect of higher maximum value a_{CUD} becomes significantly stronger. The last conclusion is also validated by the almost the same color tone presented in each of the Figs. 2-6.

In general, the belief that adding feint "smart" hooks can allow the bypass of HS-DET method is misleading. HS-DET method can detect the hook style energy theft via two or more "smart" hooks with the same difficulty as HS-DET method does when one "smart" hook is installed across the OV LV lines.

3.3 Full Interconnection Assumption, Hybrid Method and HS-DET Method Jamming

Hybrid model is extensively employed to examine the behavior of various multiconductor transmission line (MTL) configurations in transmission and distribution BPL networks [10]-[24] while it is the core element of HS-DET method. Actually, the hybrid model consists of two interconnected modules, namely: (i) the bottom-up approach module; and (ii) the top-down approach module. The top-down approach module of the hybrid model is based on the concatenation of multidimensional transmission matrices of the cascaded network BPL connections and, among others, through its interconnection multidimensional transmission matrix $\mathbf{C}_k$ describes the connection between the distribution and branch TLs (i.e., the interconnection between the phases and the neutral of two TLs) [10].

Until now [1], [2], full interconnections between the hook and the distribution TLs have been considered while the impact of partial interconnection (*i.e.,* hook hung on one phase) is here investigated. The full interconnection allows the hook to be treated as a branch by the hybrid model and, hence, the simplicity of the analysis is enhanced. To proceed with the partial interconnection, the hook is assumed to be hung only on one phase, say phase A or the green conductor of Fig. 1 of [1]. As it is obvious, the partial interconnection is more realistic way of hook style energy theft while this may have an impact on the coupling scheme that is used to detect hook style energy theft. In the case of hook hung on phase A and with reference to [10], the interconnection multidimensional transmission matrix is equal to zero array apart from the element of the first row and first column that is equal to 1.

To investigate the effect of partial interconnections during the energy theft detection by HS-DET method, with reference to Fig. 2(b) of [1] and the indicative original OV LV BPL topologies as reported in Table 1 of [1], let assume again that an open-circuit hook of length L_{bh} is inserted at distance D_{h} from the transmitting end. In Fig. 7(a), $\overline{\Delta PES}$ is plotted with respect to the maximum value a_{CUD} when $L_{\mathrm{bh}} = 5\mathrm{m}$ and $D_{\mathrm{h}} = 300\mathrm{m}$ are assumed for the five indicative original OV LV BPL topologies, hook is hung on the phase A and WtG[1] coupling scheme is applied. In Figs. 7(b) and 7(c), same curves with Fig. 7(a) are given but for the cases of WtG[2] and WtG[3] coupling schemes, respectively.

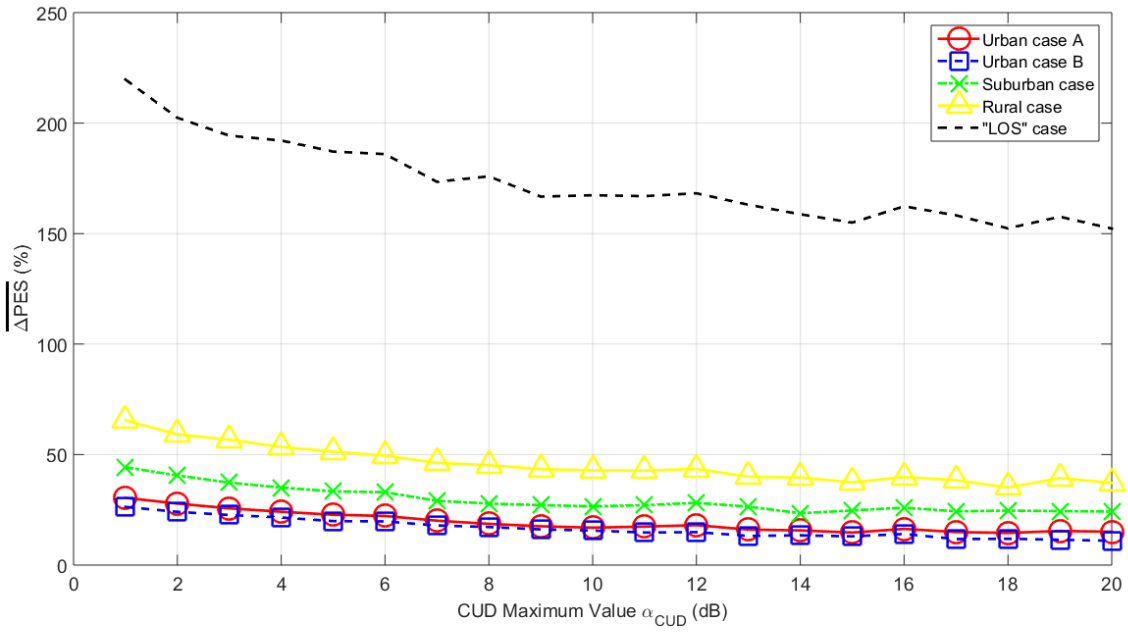
Urban case A
Urban case B
Suburban case
Rural case
"LOS" case
ΔPES (%)
CUD Maximum Value α_{CUD} (dB)

(a)

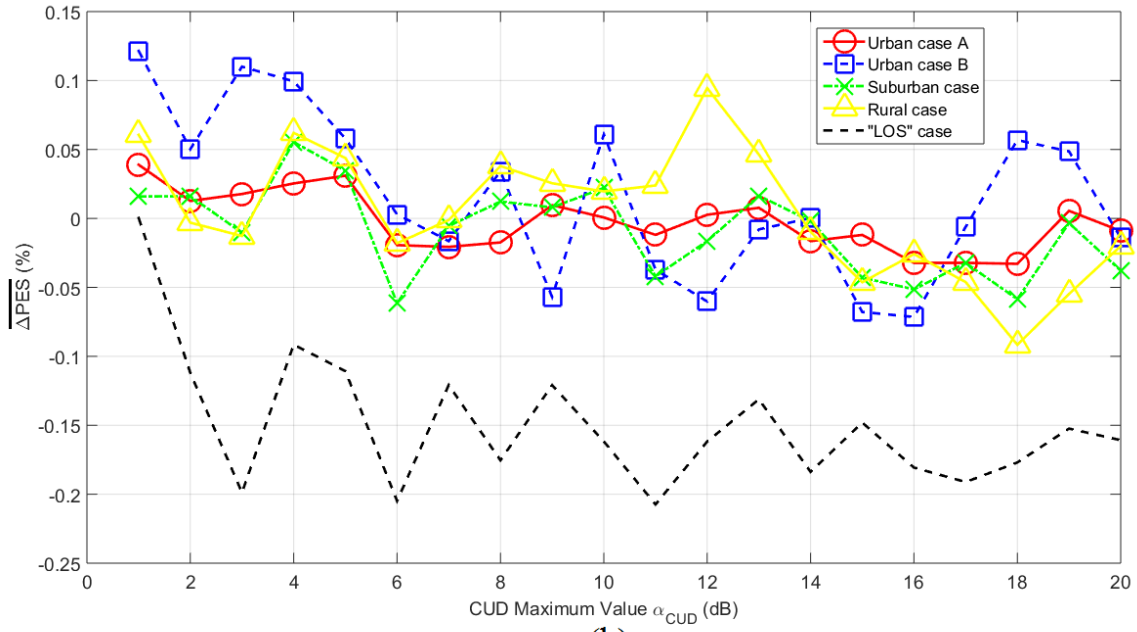
Urban case A
Urban case B
Suburban case
Rural case
"LOS" case
ΔPES (%)
CUD Maximum Value α_{CUD} (dB)

(b)

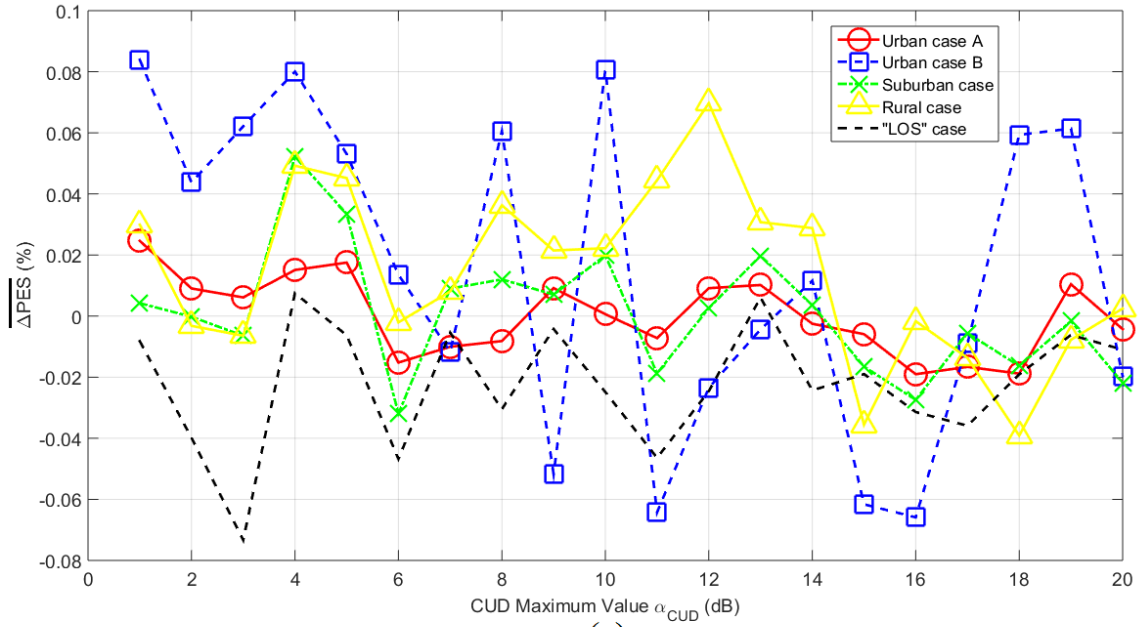

(c)

Fig. 7. $\overline{\Delta PES}$ of HS-DET method for the five original indicative OV LV BPL topologies of [1] when hook of 5m-length, of 300m-distance from the transmitting end, hung at phase A and with open-circuit termination is assumed for different WtG coupling schemes. (a) WtG[1]. (b) WtG[2]. (c) WtG[3].

From Figs. 7(a)-(c), interesting findings can be reported concerning the detection of hook style energy theft when the hook is hung on only one phase. More specifically:

- Comparing Fig. 7(a) with Fig. 1(a) of [2], $\overline{\Delta PES}$ plots are identical as expected. This means that when the applied WtG coupling scheme comprises the conductor where the hook is hung, $\overline{\Delta PES}$ plots present no differences compared with $\overline{\Delta PES}$ plots of fully interconnected hooks. Therefore, all the results of this paper, [1] and [2] occur without changes when the conductor of hook is the same with the conductor of WtG coupling scheme.
- Comparing Figs. 7(b) and 7(c) with Fig. 1(a) of [2], when the applied WtG coupling scheme does not comprise the conductor where the hook is hung, $\overline{\Delta PES}$ values are close to zero resembling with the difference measurement difference $\overline{\Delta PES}$ behavior of Fig. 8(a) of the Appendix. However, if the case of different CUD measurement differences during the determination of the original theoretical coupling scheme channel transfer function and the modified theoretical coupling scheme channel transfer function can be excluded (see Sec.2.1), the loose $\overline{\Delta PES}$ threshold may detect the hook style energy theft through the fluctuating or negative $\overline{\Delta PES}$ values even though the hook is hung on different conductor with reference to the conductor of the employed WtG coupling schemes. Therefore, with reference to Sec.2.1, a real time and continuous HS-DET method can trigger the hook style energy theft detection alarm even if the hook is hung intentionally on different conductor from the BPL injector / extractors.
- In [28]-[31], new coupling schemes for transmission and distribution BPL networks have been presented through the adoption of CS2 module. Actually, CS2 module can exploit all the available conductors of the examined MTL

configuration and, hence, the detection of the hook style energy theft can be accomplished through a periodic surveillance test of the supported multiple input multiple output (MIMO) channels.

Concluding this subsection, there are three ways of detecting the hook style energy theft when the hook is hung on only one conductor, namely: (i) through $\overline{\Delta PES}$ values when the employed WtG coupling scheme comprises the conductor where the hook is hung; (ii) through the existence of a real time and continuous HS-DET method. The exclusion of all other problematic cases can be ensured and the small $\overline{\Delta PES}$ fluctuations can imply a hook style energy theft through a different conductor from the one that is used by the applied WtG coupling scheme, and (iii) by exploiting WtW and MtM coupling schemes of CS2 module. These coupling schemes exploit all the conductors of the examined MTL configuration and, thus, the hook style energy theft detection can be easily achieved through a periodic check of the MIMO channel health.

3. Conclusions

This paper has focused on the performance of HS-DET method when the three more sophisticated scenarios of [2] are addressed. In fact, these sophisticated cases are considered as the further consideration of special cases presented in [1] and investigated in [2]. As the first sophisticated scenario has been examined, the effect of two different CUD measurement differences on $\overline{\Delta PES}$ and $\overline{Rob}$ values remains marginal in comparison with the respective $\overline{\Delta PES}$ and $\overline{Rob}$ values when one CUD measurement difference is assumed during the computation of the original theoretical coupling scheme channel transfer function and the modified theoretical coupling scheme channel transfer function. In all the cases of average values of CUD maximum values $a_{\mathbf{CUD}}$, the hook style energy theft has been detected by HS-DET method through strict $\overline{\Delta PES}$ and $\overline{Rob}$ thresholds. As the second sophisticated scenario has been investigated, HS-DET method more easily detects the energy theft when a second "smart" hook, either acting as a feint "smart" hook or not, is installed across OV LV TLs. In fact, $\overline{\Delta PES}$ values for given OV LV BPL topology with two "smart" hooks are significantly higher than the respective ones of the same OV LV BPL topology with one "smart" hook regardless of the distance between them. Hence, by generalizing the findings of two "smart" hooks, the myth of many "smart" hooks that can jam HS-DET method has been disproven. The third sophisticated scenario that has been examined was the impact of the assumption of full interconnections during the computations of HS-DET method. When the hook is hung on only one conductor, three different detection cases have been analyzed that allow HS-DET method to securely detect the hook style energy theft. The three special cases of [1] and the three sophisticated scenarios of this paper have aimed at jamming HS-DET method. As it has been proven, HS-DET method can detect all the potential hook style energy thefts in OV LV BPL networks through its strict $\overline{\Delta PES}$ threshold in the vast majority of the cases and its loose $\overline{\Delta PES}$ threshold in few aggravated cases. Finally, the virtue of maintaining a real-time and continuous HS-DET method combined with CS2 module conveniences has been praised and its advantages have been analytically reported.

Appendix – Can Different CUD Measurement Differences Trigger the Hook Style Energy Theft Alarm of HS-DET Method

The impact of same CUD measurement difference during the determination of the original measured coupling scheme channel transfer function and the modified measured coupling scheme channel transfer functions on $\overline{\Delta PES}$, $\overline{PES_{or}}$ and $\overline{Rob}$ has been examined in the Appendix of [2]. In this Appendix, the sole influence of different CUD measurement differences but of the same maximum value $a_{\mathbf{CUD}}$ during the determination of the original measured coupling scheme channel transfer function and the modified measured coupling scheme channel transfer functions on the aforementioned three PES submetrics is evaluated. With reference to eqs (3)-(8) of [1], the modified theoretical coupling scheme channel transfer function $H_{\mathbf{mod}}^{\mathbf{C}}\{\cdot\}$ is assumed to be equal to the original theoretical coupling scheme channel transfer function $H_{\mathbf{or}}^{\mathbf{C}}\{\cdot\}$. With reference to eqs. (5) and (6) of [1], since different measurement differences are considered, $\overline{PES_{or}}$ stops being equal to $\overline{PES_{mod}}$ when the aforementioned assumption occurs. In general terms, the critical issue now is the difference between the two assumed CUD measurement differences for given frequency.

To examine the impact of the two different CUD measurement differences of the same maximum value $a_{\mathbf{CUD}}$, in Fig. 8(a), $\overline{\Delta PES}$ is plotted with respect to the maximum value $a_{\mathbf{CUD}}$ when the modified OV LV BPL topology is assumed to be the same with the original one for the five indicative original OV LV BPL topologies of Table 1 of [1]. Note that two different CUD measurement differences of the same maximum value $a_{\mathbf{CUD}}$ are used during the determination of the original measured coupling scheme channel transfer function and the modified measured coupling scheme channel transfer functions. In Figs. 8(b) and 8(c), same curves with Fig. 8(a) are given but for $\overline{PES_{or}}$ and $\overline{Rob}$, respectively.

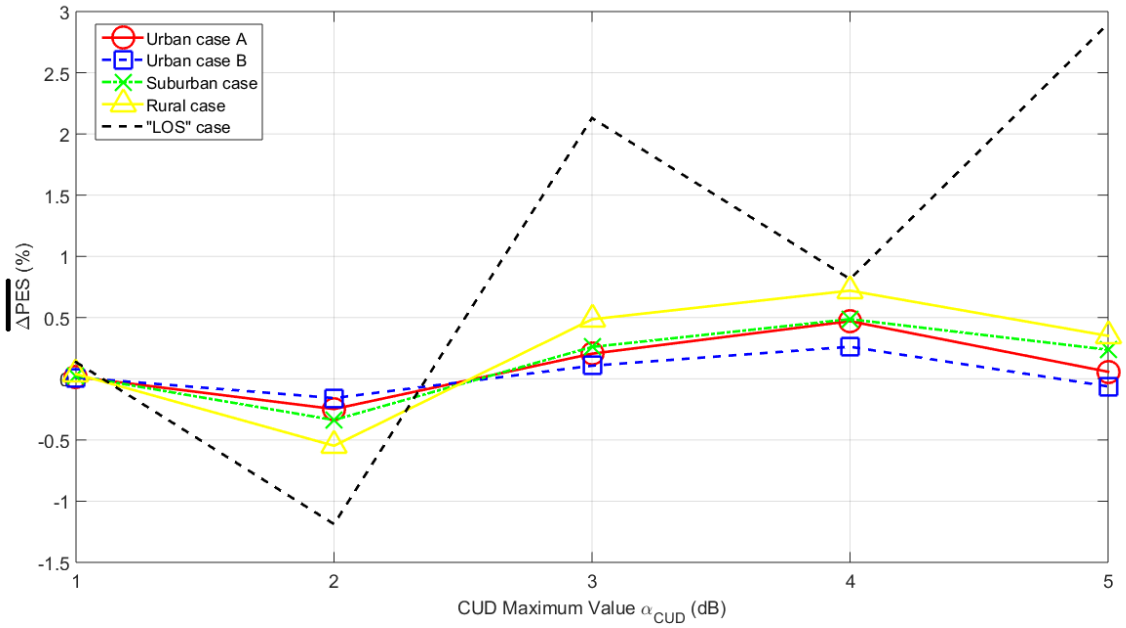
Urban case A
Urban case B
Suburban case
Rural case
"LOS" case
ΔPES (%)
CUD Maximum Value α_{CUD} (dB)

(a)

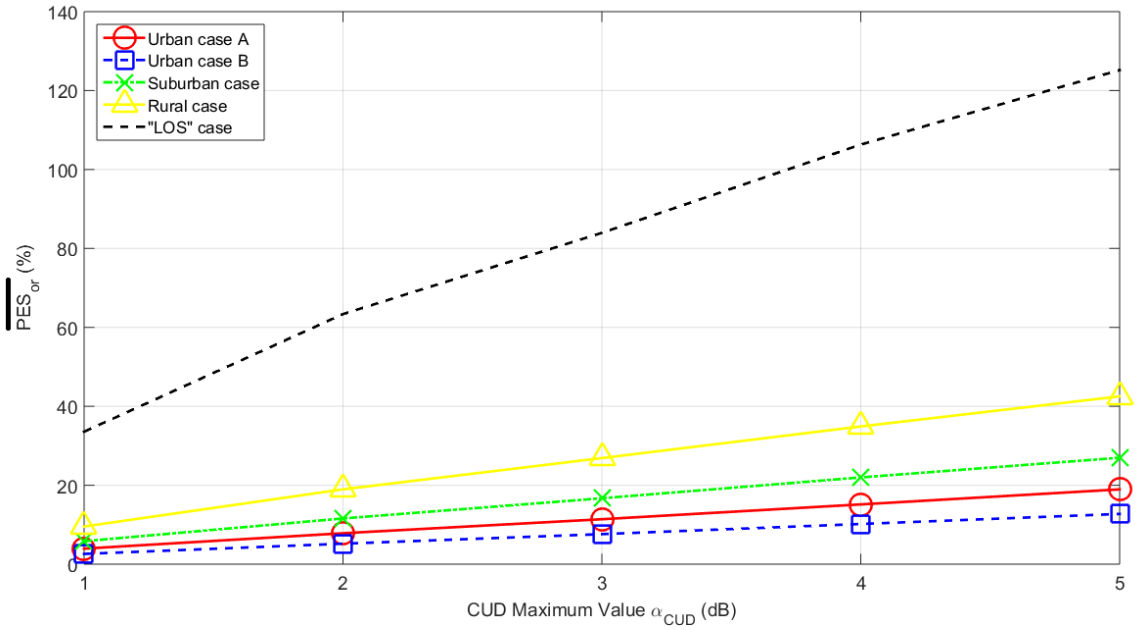
Urban case A
Urban case B
Suburban case
Rural case
"LOS" case
PES_{or} (%)
CUD Maximum Value α_{CUD} (dB)

(b)

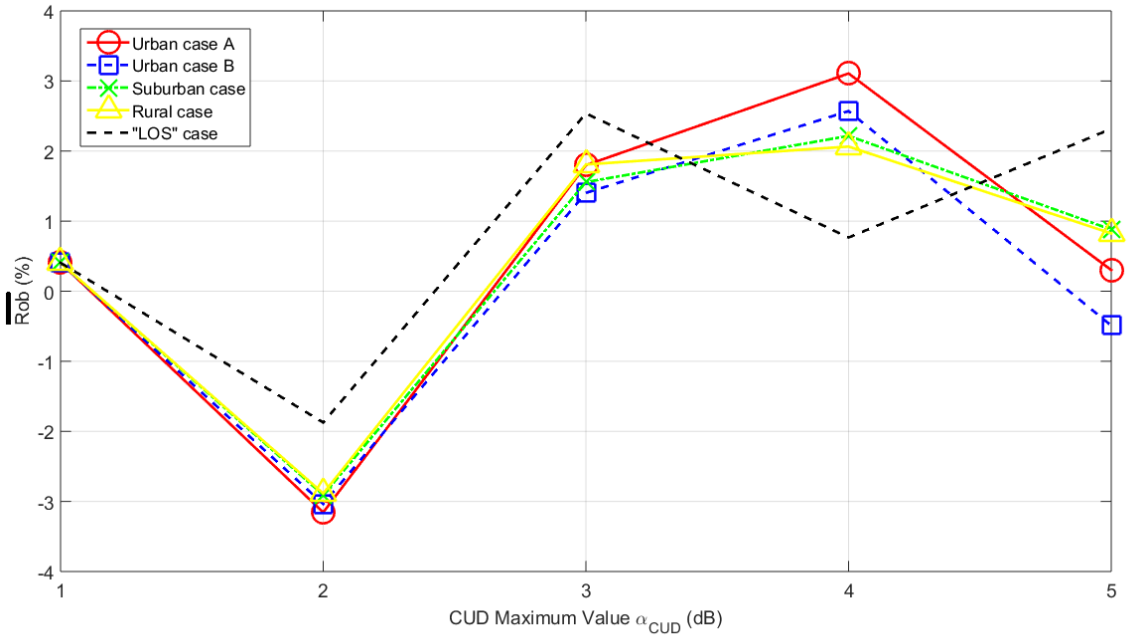

(c)

Fig. 8. PES submetrics of HS-DET method for the five original indicative OV LV BPL topologies of [1] when modified OV LV BPL topology is assumed the same with the original one and two different CUD measurement differences and various maximum values a_{CUD}. (a) $\overline{\Delta PES}$. (b) $\overline{PES_{or}}$. (c) $\overline{Rob}$.

By comparing Figs. 8(a)-(c) with the findings of [2], the following conclusions can be deduced concerning $\overline{\Delta PES}$, $\overline{PES_{or}}$ and $\overline{Rob}$, say:

- Due to the definition of $\overline{\Delta PES}$ and $\overline{Rob}$, their study is focused on weighted differences between the absolute values of different CUD measurement differences of the same maximum value a_{CUD} since the modified theoretical coupling scheme channel transfer function and the original theoretical coupling scheme channel transfer function are equal. Therefore, it is expected that $\overline{\Delta PES}$ and $\overline{Rob}$ behave as CUD variables of zero mean. Possible divergences are due to the weighted definition of $\overline{\Delta PES}$ and $\overline{Rob}$.
- Already been mentioned in [2], $\overline{PES_{or}}$ is independent of the modified measured coupling scheme channel transfer function since it depends only on the original measured and original theoretical coupling scheme channel transfer function. Hence, the increase of the considered maximum value a_{CUD} is reflected on the increased values of $\overline{PES_{or}}$.
- The influence of the different CUD measurement differences to $\overline{\Delta PES}$ and $\overline{Rob}$ values remain marginal and significantly lower than the respective strict $\overline{\Delta PES}$ and $\overline{Rob}$ thresholds. However, $\overline{\Delta PES}$ and $\overline{Rob}$ values render precarious such a decision based on the loose $\overline{\Delta PES}$ and $\overline{Rob}$ thresholds.

Concluding this Appendix, the effect of two different CUD measurement differences on $\overline{\Delta PES}$ and $\overline{Rob}$ values remains marginal allowing the decision concerning the existence of hook style energy theft by using the respective strict $\overline{\Delta PES}$ and $\overline{Rob}$ thresholds. However, the cost of a non-real time and continuous HS-DET method in

terms of $\overline{\Delta PES}$ and $\overline{Rob}$ is that decisions concerning the hook style energy theft that are based on the loose $\overline{\Delta PES}$ and $\overline{Rob}$ can be considered as risky ones.

CONFLICTS OF INTEREST

The author declares that there is no conflict of interests regarding the publication of this paper.

References

[1] A. G. Lazaropoulos, "Detection of Energy Theft in Overhead Low-Voltage Power Grids – The Hook Style Energy Theft in the Smart Grid Era," *Trends in Renewable Energy*, vol. 5, no. 1, pp. 12 – 46, Oct. 2018. [Online]. Available: http://futureenergysp.com/index.php/tre/article/view/81/pdf

[2] A. G. Lazaropoulos, "Special Cases during the Detection of the Hook Style Energy Theft in Overhead Low-Voltage Power Grids through HS-DET Method – Part 1: High Measurement Differences, Very Long Hook Technique and "Smart" Hooks," *Trends in Renewable Energy*, vol. 5, no. 1, pp. 60 – 89, Dec. 2018. DOI: 10.17737/tre.2019.5.1.0082

[3] A. G. Lazaropoulos, "Measurement Differences, Faults and Instabilities in Intelligent Energy Systems – Part 1: Identification of Overhead High-Voltage Broadband over Power Lines Network Topologies by Applying Topology Identification Methodology (TIM)," *Trends in Renewable Energy*, vol. 2, no. 3, pp. 85 – 112, Oct. 2016. [Online]. Available: http://futureenergysp.com/index.php/tre/article/download/26/32

[4] A. G. Lazaropoulos, "Measurement Differences, Faults and Instabilities in Intelligent Energy Systems – Part 2: Fault and Instability Prediction in Overhead High-Voltage Broadband over Power Lines Networks by Applying Fault and Instability Identification Methodology (FIIM)," *Trends in Renewable Energy*, vol. 2, no. 3, pp. 113 – 142, Oct. 2016. [Online]. Available: http://futureenergysp.com/index.php/tre/article/view/27/33

[5] A. G. Lazaropoulos, "Power Systems Stability through Piecewise Monotonic Data Approximations – Part 2: Adaptive Number of Monotonic Sections and Performance of L1PMA, L2WPMA and L2CXCV in Overhead Medium-Voltage Broadband over Power Lines Networks," *Trends in Renewable Energy*, vol. 3, no. 1, pp. 33 – 60, Jan. 2017. [Online]. Available: http://futureenergysp.com/index.php/tre/article/view/30/35

[6] A. G. Lazaropoulos, "Power Systems Stability through Piecewise Monotonic Data Approximations – Part 1: Comparative Benchmarking of L1PMA, L2WPMA and L2CXCV in Overhead Medium-Voltage Broadband over Power Lines Networks," *Trends in Renewable Energy*, vol. 3, no. 1, pp. 2 – 32, Jan. 2017. [Online]. Available: http://futureenergysp.com/index.php/tre/article/view/29/34

[7] A. G. Lazaropoulos, "Main Line Fault Localization Methodology in Smart Grid – Part 1: Extended TM2 Method for the Overhead Medium-Voltage Broadband over Power Lines Networks Case," *Trends in Renewable Energy*, vol. 3, no. 3, pp. 2-25,

Dec. 2017. [Online]. Available: http://futureenergysp.com/index.php/tre/article/view/36

[8] A. G. Lazaropoulos, "Main Line Fault Localization Methodology in Smart Grid – Part 2: Extended TM2 Method, Measurement Differences and L1 Piecewise Monotonic Data Approximation for the Overhead Medium-Voltage Broadband over Power Lines Networks Case," *Trends in Renewable Energy*, vol. 3, no. 3, pp. 26-61, Dec. 2017. [Online]. Available: http://futureenergysp.com/index.php/tre/article/view/37

[9] A. G. Lazaropoulos, "Main Line Fault Localization Methodology in Smart Grid – Part 3: Main Line Fault Localization Methodology (MLFLM)," *Trends in Renewable Energy*, vol. 3, no. 3, pp. 62-81, Dec. 2017. [Online]. Available: http://futureenergysp.com/index.php/tre/article/view/38

[10] A. G. Lazaropoulos, "Towards Modal Integration of Overhead and Underground Low-Voltage and Medium-Voltage Power Line Communication Channels in the Smart Grid Landscape: Model Expansion, Broadband Signal Transmission Characteristics, and Statistical Performance Metrics (Invited Paper)," *ISRN Signal Processing*, vol. 2012, Article ID 121628, pp. 1-17, 2012. [Online]. Available: http://www.hindawi.com/isrn/sp/2012/121628/

[11] A. G. Lazaropoulos, "Towards broadband over power lines systems integration: Transmission characteristics of underground low-voltage distribution power lines," *Progress in Electromagnetics Research B*, 39, pp. 89-114, 2012. [Online]. Available: http://www.jpier.org/PIERB/pierb39/05.12012409.pdf

[12] A. G. Lazaropoulos and P. G. Cottis, "Transmission characteristics of overhead medium voltage power line communication channels," *IEEE Trans. Power Del.*, vol. 24, no. 3, pp. 1164-1173, Jul. 2009.

[13] A. G. Lazaropoulos and P. G. Cottis, "Capacity of overhead medium voltage power line communication channels," *IEEE Trans. Power Del.*, vol. 25, no. 2, pp. 723-733, Apr. 2010.

[14] A. G. Lazaropoulos and P. G. Cottis, "Broadband transmission via underground medium-voltage power lines-Part I: transmission characteristics," *IEEE Trans. Power Del.*, vol. 25, no. 4, pp. 2414-2424, Oct. 2010.

[15] A. G. Lazaropoulos and P. G. Cottis, "Broadband transmission via underground medium-voltage power lines-Part II: capacity," *IEEE Trans. Power Del.*, vol. 25, no. 4, pp. 2425-2434, Oct. 2010.

[16] A. G. Lazaropoulos, "Broadband transmission characteristics of overhead high-voltage power line communication channels," *Progress in Electromagnetics Research B*, vol. 36, pp. 373-398, 2012. [Online]. Available: http://www.jpier.org/PIERB/pierb36/19.11091408.pdf

[17] A. G. Lazaropoulos, "Green Overhead and Underground Multiple-Input Multiple-Output Medium Voltage Broadband over Power Lines Networks: Energy-Efficient Power Control," *Springer Journal of Global Optimization*, vol. 2012 / Print ISSN 0925-5001, pp. 1-28, Oct. 2012.

[18] A. G. Lazaropoulos, "Deployment Concepts for Overhead High Voltage Broadband over Power Lines Connections with Two-Hop Repeater System: Capacity Countermeasures against Aggravated Topologies and High Noise Environments," *Progress in Electromagnetics Research B*, vol. 44, pp. 283-307, 2012. [Online]. Available: http://www.jpier.org/PIERB/pierb44/13.12081104.pdf

[19] A. G. Lazaropoulos, "Broadband transmission and statistical performance properties of overhead high-voltage transmission networks," *Hindawi Journal of Computer Networks and Commun.*, 2012, article ID 875632, 2012. [Online]. Available: http://www.hindawi.com/journals/jcnc/aip/875632/

[20] P. Amirshahi and M. Kavehrad, "High-frequency characteristics of overhead multiconductor power lines for broadband communications," *IEEE J. Sel. Areas Commun.*, vol. 24, no. 7, pp. 1292-1303, Jul. 2006.

[21] T. Calliacoudas and F. Issa, ""Multiconductor transmission lines and cables solver," An efficient simulation tool for plc channel networks development," presented at the *IEEE Int. Conf. Power Line Communications and Its Applications*, Athens, Greece, Mar. 2002.

[22] T. Sartenaer and P. Delogne, "Deterministic modelling of the (Shielded) outdoor powerline channel based on the multiconductor transmission line equations," *IEEE J. Sel. Areas Commun.*, vol. 24, no. 7, pp. 1277-1291, Jul. 2006.

[23] C. R. Paul, *Analysis of Multiconductor Transmission Lines*. New York: Wiley, 1994.

[24] H. Meng, S. Chen, Y. L. Guan, C. L. Law, P. L. So, E. Gunawan, and T. T. Lie, "Modeling of transfer characteristics for the broadband power line communication channel," *IEEE Trans. Power Del.*, vol. 19, no. 3, pp. 1057-1064, Jul. 2004.

[25] B. Li, D. Mansson, and G. Yang, "An efficient method for solving frequency responses of power-line networks," *Progress in Electromagnetics Research B*, Vol. 62, 303-317, 2015. DOI: 10.2528/PIERB15013008 http://www.jpier.org/pierb/pier.php?paper=15013008

[26] M. Chaaban, K. El KhamlichiDrissi, and D. Poljak, "Analytical model for electromagnetic radiation by bare-wire structures," *Progress in Electromagnetics Research B*, Vol. 45, 395-413, 2012. DOI:10.2528/PIERB12091102 http://www.jpier.org/pierb/pier.php?paper=12091102

[27] Y. H. Kim, S. Choi, S. C. Kim, and J. H. Lee, "Capacity of OFDM two-hop relaying systems for medium-voltage power-line access networks," *IEEE Trans. Power Del.*, vol. 27, no. 2, pp. 886-894, Apr. 2012.

[28] A. G. Lazaropoulos, "New Coupling Schemes for Distribution Broadband over Power Lines (BPL) Networks," *Progress in Electromagnetics Research B*, vol. 71, pp. 39-54, 2016. [Online]. Available: http://www.jpier.org/PIERB/pierb71/02.16081503.pdf

[29] A. G. Lazaropoulos, "Broadband Performance Metrics and Regression Approximations of the New Coupling Schemes for Distribution Broadband over Power Lines (BPL) Networks," *Trends in Renewable Energy*, vol. 4, no. 1, pp. 43 – 73, 2018. [Online]. Available: http://www.futureenergysp.com/index.php/tre/article/view/59/pdf

[30] A. G. Lazaropoulos, "Smart Energy and Spectral Efficiency (SE) of Distribution Broadband over Power Lines (BPL) Networks – Part 1: The Impact of Measurement Differences on SE Metrics," *Trends in Renewable Energy*, vol. 4, no. 2, pp. 125-184, Aug. 2018. [Online]. Available: http://futureenergysp.com/index.php/tre/article/view/76/pdf

[31] A. G. Lazaropoulos, "Smart Energy and Spectral Efficiency (SE) of Distribution Broadband over Power Lines (BPL) Networks – Part 2: L1PMA, L2WPMA and L2CXCV for SE against Measurement Differences in Overhead Medium-Voltage BPL Networks," *Trends in Renewable Energy*, vol. 4, no. 2, pp. 185-212, Aug.

2018. [Online]. Available: http://futureenergysp.com/index.php/tre/article/view/77/pdf